Lithium ion-inserted TiO$_2$ nanotube array photoelectrocatalysts

Unseock Kang, Hyunwoong Park *

School of Energy Engineering, Kyungpook National University, Daegu 702-701, South Korea

A B S T R A C T

A quick electrochemical Li ion insertion into TiO$_2$ nanotube arrays (TNTs) markedly enhances the photo-electrochemical and photoelectrocatalytic performance. Potential pulses ($-1.0 \sim -1.7\,\mathrm{V_{SCE}}$ for 1–11 s in 1 M LiClO$_4$) to pre-annealed TNTs effectively insert Li ions (pre-annealed Li-TNTs) into the mouth/wall and bottom TiO$_2$ depending on the insertion condition. Pre-annealed Li-TNTs prepared under an optimal Li ion insertion condition ($-1.4\,\mathrm{V_{SCE}}$ for 3 s) exhibit $\sim$70%-enhanced photocurrent generation, $\sim$2.5 fold-higher incident photon-to-current efficiency, and an improved photoelectrocatalytic activity for the degradation of phenolic compounds in 1 M KOH electrolyte. A change in photoluminescence (PL) emission spectra and decrease in charge transfer resistance by Li ion insertion suggest that the inserted Li ions play a role in inhibiting charge recombination by compensating for the photogenerated Ti^{3+} charges (Li$^+$-Ti^{3+}-OH). However, as KOH concentration is diluted such enhanced Li$^+$ effects gradually vanish primarily due to liberation of reversibly inserted Li ions. To insert Li ions irreversibly, the potential pulses were applied to non-annealed TNTs followed by annealing (post-annealed Li-TNTs). Comparison between pre-annealed and post-annealed Li-TNTs in circum-neutral pH (0.1 M Na$_2$SO$_4$ at pH $\sim$6) indicates that the former exhibits a similar performance to bare TNTs (absence of Li ion effect), whereas the latter shows a superior performance with ca. 2.5-fold higher photoelectrochemical and photoelectrocatalytic activities. Detailed surface analyses (XPS, XRD, PL, SEM, ICP-MS, etc.) and Li$^+$-induced reaction mechanism were discussed.

© 2013 Elsevier B.V. All rights reserved.

1. Introduction

TiO$_2$ nanotube arrays (TNTs) grown on titanium foil through electrochemical anodization have attracted great attention as a light harvesting 1-D scaffold [1,2]. The self-standing, aligned 1-D architecture is beneficial for photogenerated electron transport along the tube framework leaving holes on the surface [1,3–6]. In addition, the tubular structure provides a unique submicron-sized environment where a variety of metals, semiconductors, and molecules are selectively located for a further increase in the photoelectrochemical performance and various applications [7–12]. Despite such geometric uniqueness and photoelectrocatalytic superiority compared to TiO$_2$ nanoparticles (TNPs), however, TNTs still suffers from inherent charge recombination [4,10,13–15], limiting their further application Scheme 1.

Recently, Li ion insertion into TiO$_2$ has received growing attention since the Li-battery industry has rapidly grown [16–21]. The insertion is simply achieved by applying negative potentials to TiO$_2$ electrodes in a Li$^+$-rich solution (reaction (1)):

$$> \mathrm{TiO_2} + x\mathrm{e}^- + x\mathrm{Li}^+ \rightarrow \; > \mathrm{Li}_x\mathrm{TiO_2} \qquad (1)$$
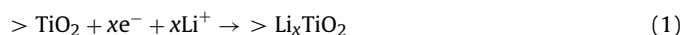
A sufficiently high negative bias potential supplies excess electrons to the TiO$_2$ conduction band (CB) increasing capacitance and conductivity [22], as well as inducing upward band-bending and an accumulation regime in TiO$_2$. The accumulation of negative charges (i.e., $\rangle$Ti^{3+}-OH) is then effectively compensated by Li$^+$ insertion ($\rangle$Ti^{3+}Li$^+$-OH) [20]. A crystallographic study estimated that there are channels with a minimum diameter of 0.07 nm in TiO$_2$ [23], making Li ion (ionic diameter $\sim$ 0.068 nm) insertion inherently possible. Electrochemical Li ion insertion is favored by small and anatase TiO$_2$ particles [24,25], and creates new Ti 2p states (Ti^{3+}) along with changed O1s states due to the formation of Li$_2$O/LiOH [26]. Treatment of TiO$_2$ with Li ions shifts the Fermi level (E_F) upward due to the lithium oxide/hydroxide dipole layers ($\rangle$Ti-O$^-$-Li$^+$), improving the photovoltages in dye-sensitized solar cells [27].

It is surprising that despite a number of papers on Li$^+$-inserted TiO$_2$ (Li-TiO$_2$), its photoelectrocatalytic behavior has been hardly reported. Very recently, Meekins and Kamat showed that Li ion insertion significantly enhances the photoelectrochemical efficiency of TNTs in highly Li$^+$-rich or alkaline solutions [28]. The high efficiency Li-TNTs was attributed primarily to inhibited charge recombination by blocking electron trap sites. Two challenging issues remain unsolved. Firstly, if the enhanced photoelectrochemical efficiency truly resulted from the Li$^+$-inhibited charge recombination, hole-mediated photocatalytic activities also should be enhanced because the inhibited charge recombination should

* Corresponding author. Tel.: +82 53 950 8973.
  E-mail address: hwp@knu.ac.kr (H. Park).
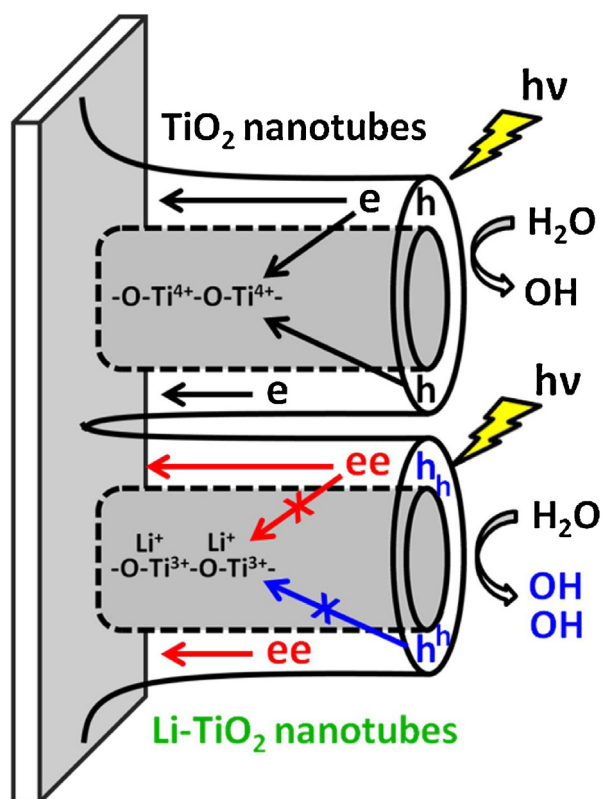
Scheme 1. Schematic illustration of photogenerated charge transfers in bare and Li ion-inserted TiO$_2$ nanotube arrays.

result in more generation of holes (or hydroxyl radicals). However, contrary results were reported by other groups that the photocatalytic activity of Li-TiO$_2$ particles is decreased for the decomposition of organic chemicals [29,30]. Secondly, the photoelectrochemical stability of Li-TNTs must be guaranteed for practical application. Unfortunately, the inserted Li ions tend to leach out from TNTs at circum-neutral and acidic pH because protons competes with Li ions for TNTs.

The objective of this study is to investigate if Li ion insertion enhances photoelectrochemical charge transfers occurring on TNTs, and as a result, increases its photoelectrocatalytic performance for degradation of organic compounds. For this objective, Li ions are inserted in TNTs in pre-annealed TNTs. Because this type of TNTs is crystallized prior to Li ion insertion, the post-inserted Li ions are exchangeable with protons (i.e., reversible Li$^+$ insertion) and preserved in the TNTs only in alkaline conditions (see reaction (4)). The Li ion effects are found to be very promising for photocurrent generation and photoelectrocatalytic degradation of organic compounds, but the effects disappear with decreasing KOH concentration. Alternatively, when Li ions are inserted into non-annealed TNTs followed by post-annealing, the enhanced Li$^+$ effects are preserved even in circum-neutral pH conditions.

2. Experimental

2.1. Preparation of bare and Li-inserted TiO$_2$ nanotubes

TNTs were prepared by following a modified anodization method of titanium (Ti) foils in a two-electrode system [10]. A titanium sheet (0.127 mm thick, 99.7%-pure, Aldrich) was cut into small pieces with equal size 1.5 × 3.0 cm^2, which were ultrasonically cleaned in ethanol for 10 min in a sonicaiton bath (WiseClean, 40 kHz, 100 W) and rinsed with deionized water. A couple of a Ti

foil piece and a stainless steel plate was immersed in a mixed aqueous solution of NaF (0.28 M) and H$_3$PO$_4$ (1.0 M) and a dc voltage of +20 V was applied to the Ti foil (anode) against the stainless steel (cathode) for 4 h with magnetic stirring. Then, the Ti foil piece was annealed at 500 °C for 6 h in the presence of air (pre-annealed TNTs). For Li insertion, the pre-annealed TNTs were immersed in 1 M LiClO$_4$ and negative potentials ranging between −1.0 and −1.7 V was pulsed against a saturate calomel electrode (SCE, reference electrode) for varying times (3–12 s) using a potentiostat (Versastat 3-400). Then, the TNTs were rinsed with deionized water and dried in air (hereafter pre-annealed Li-TNTs). Alternatively, non-annealed TNTs were used for Li insertion under the same electrochemical condition, and then they were annealed at 500 °C for 6 h in the presence of air (post-annealed Li-TNTs). For comparison, bare Ti foils were annealed at 500 °C for 6 h to grow TiO$_2$ nanoparticles on Ti foils (TNPs), followed by Li insertion.

2.2. Photoelectrochemical and photoelectrocatalytic activity tests

The photoelectrochemical activities of TNTs and Li-TNTs were studied in a three-electrode system with SCE and graphite rod as a reference and a counter electrode, respectively, in various electrolytes ((NH$_4$)$_2$SO$_4$, Na$_2$SO$_4$, or KOH) using a potentiostat (Versastat 3-400). A 150 W-Xenon arc lamp (Ushio 150-MO) equipped with an AM 1.5G air mass filter was used as a light source. The incident photon-to-current efficiency (IPCE) or external quantum efficiency (EQE) was estimated in 1 M KOH with the same three-electrode system using a 300 W-Xenon lamp (Newport Oriel). Monochromatic light was produced by a CS 130 monochromator with a 10 nm-bandpass, and the output power was measured with a silicon photodiode detector (Newport). The IPCE was then calculated from $(1240 \times J_{ph}) \times 100/(P_{light} \times \lambda)$, where J_{ph} (mA/cm^2), P_{light} (mW/cm^2), and λ (nm) refer to the photocurrent density at 1.0 V$_{SCE}$, photon flux, and wavelength, respectively. For the impedance analysis (Nyquist plots), alternating current (AC) impedance measurements were carried out through application of a bias potential of −0.3 V$_{SCE}$ in 1 M KOH solution with a frequency range of 10 MHz to 0.01 Hz and an AC voltage of 10 mV rms (Gamry Instruments) [31,32]. For the photoelectrocatalytic activity, as-prepared TNTs and Li-TNTs were immersed in aqueous solutions of phenol (50 and 100 μM), triclosan (0.1 mM), and N,N-dimethyl-p-nitrosoaniline (RNO, 0.1 mM), and the AM 1.5-light was irradiated to the front side of the electrodes through the solutions. The concentrations and intermediates of phenol and triclosan were analyzed with a high performance liquid chromatography (HPLC, YL9100). The mixed eluent with distilled water (with 0.1 wt.% phosphoric acid) and acetonitrile (55/45 v/v) was flowed through a C18-inverse column (4.6 mm × 150 mm) at 1 mL/min. RNO was quantified by recording its main absorption band at 440 nm using a UV–vis spectrophotometer (PerkinElmer, Lambda 950) [33].

2.3. Surface characterization

X-ray diffractometer (XRD, Rigaku D/Max-2500) and X-ray photoelectron spectroscopy (XPS, VG scientific, ESCA LAB 220i XL, MgKα source) were employed to examine crystalline patterns and binding states of sample elements, respectively. Inductively coupled plasma (ICP, PerkinElmer Optima 7300DV) was used to quantify inserted Li ions. Field emission scanning electron microscope (FE-SEM, Hitachi S-4800) was also employed to analyze the morphologies of TNTs and Li-TNTs. Photoluminescence spectra were recorded at room temperature using a spectrometer (f = 0.5 m, Acton Research Co., Spectrograph 500i, U.S.A.) equipped with an intensified photodiode array detector (Princeton Instrument Co., IRY1024, U.S.A.). A He-Cd laser (Kimmon, 1 K, Japan)